PeV–EeV neutrinos from GRB blastwave in IceCube and future neutrino telescopes

Soebur Razzaque[1,*] and Lili Yang[1,2,†]

[1] *Department of Physics, University of Johannesburg, PO Box 524, Auckland Park 2006, South Africa*

[2] *Laboratory for Astroparticle Physics, University of Nova Gorica, Vipavska 13, 5000 Nova Gorica, Slovenia*

(Dated: January 20, 2015)

Ultrahigh-energy cosmic rays (UHECRs), if accelerated in the gamma-ray burst (GRB) blastwave, are expected to produce PeV–EeV neutrinos by interacting with long-lived GRB afterglow photons. Detailed spectral and temporal properties of the flux of these neutrinos depend on the GRB blastwave evolution scenario, but can last for days to years time scale in contrast to the seconds to minutes time scale for "burst" neutrino flux contemporaneous with the prompt gamma-ray emission and which has been constrained by IceCube in the $\sim$ 50 TeV–2 PeV range. We compute expected neutrino events in IceCube in the PeV–EeV range from the blastwave of long-duration GRBs, both for the diffuse flux and for individual GRBs in the nearby universe. We show that IceCube will be able to detect the diffuse GRB blastwave neutrino flux after 5 years of operation, and will be able to distinguish it from the cosmogenic neutrino flux arising from GZK process in case the UHECRs are heavy nuclei. We also show that EeV neutrinos from the blastwave of an individual GRB can be detected with long-term monitoring by a future high-energy extension of IceCube for redshift up to $z \sim 0.5$.

PACS numbers: 95.85.Ry, 98.70.Sa, 14.60.Pq

arXiv:1411.7491v2 [astro-ph.HE] 18 Jan 2015

I. INTRODUCTION

The long-duration gamma-ray bursts are thought to be the sources of ultrahigh-energy cosmic rays ($\gtrsim 10^{18}$ eV) in nature [1, 2]. Acceleration of protons and/or ions to ultrahigh energies can take place in the internal shocks and/or external forward and reverse shocks. In cases of internal and external reverse shocks, GRB jets must contain protons and/or ions in the form of ejected material from the GRB central engine [3]. In case of external forward shock, which is responsible for GRB afterglow emission [4], protons and/or ions from circumburst medium, forming a blastwave, are accelerated. Interactions of ultrahigh-energy particles (assumed dominated by protons) with the ambient prompt or afterglow photons via $p\gamma \to \pi^{\pm}$, $K^{\pm}$ processes are expected to produce ν from decays such as $\pi^+/K^+ \to \mu^+\nu_\mu \to e^+\nu_e\bar{\nu}_\mu\nu_\mu$ [49]. Detection of these ν can identify GRBs as accelerators of UHECRs.

IceCube Neutrino Observatory has recently imposed constraining limits on the GRB "burst" ν flux [6–10] in the $\sim$ 50 TeV–2 PeV range [11]. The ANTARES neutrino telescope has also imposed somewhat weaker limits on the same flux [12]. The most recent IceCube GRB analysis [13] also constrains neutrino flux from a model for prompt γ-ray emission alternate to the internal shocks model [14]. Such limits are extremely useful to understand the content of the GRB jet, its velocity and distance of the γ-ray emission region from the central engine. Non-detection of ν from a recent, bright burst GRB 130427A [15] at relatively low redshift ($z = 0.34$) led to interesting constraints on the emission radius and the bulk Lorentz factor (Γ) of the GRB jet [16]. Detection of γ rays, with energy exceeding 10 GeV, from many GRBs by the Large Area Telescope (LAT) onboard the *Fermi Gamma Ray Space Telescope* also implies that $\Gamma \gg 100$ (see, e.g., Ref. [17, 18]), to avoid *in-situ* $\gamma\gamma \to e^{\pm}$ pair production. The fraction of Fermi-LAT GRBs is of the order of 10% of the rate of GRBs detected by the gamma-ray burst monitor (GBM) onboard Fermi [18].

Ultrahigh-energy proton interactions ($p\gamma$) in the GRB blastwave can produce PeV–EeV neutrinos [19–22]. These ν can be produced efficiently and for a much longer time scale, if the blastwave has a high initial bulk Lorentz factor [21], as compared to the PeV–EeV ν from reverse shock [23–25] which may be absent if the GRB jet is magnetic energy dominated. In case GRBs are not the significant sources of observed UHECRs, these ν can still probe baryon loading, magnetic field, particle acceleration, etc. in the GRB jet. Here we calculate expected ν flux from GRB blastwave and the event rates in IceCube using diffuse flux from all GRBs in the history of the universe. We compare these rates with those from the cosmogenic ν flux arising from GZK processes. We also calculate ν events from individual GRB blastwaves in nearby universe ($z \lesssim 0.5$) and the rate of detecting GRBs in ν by IceCube. Finally, we estimate event rates for the GRB blastwave ν fluxes by the proposed high-energy upgrade of IceCube, which we refer to as IceHEX, that will increase effective area in the $\gtrsim 1$ PeV range by up to two orders of magnitude [26].

We describe our ν flux model calculations in Sec. II and calculate ν detection rates by IceCube and IceHEX in Sec III. We discuss our results and draw conclusions in Sec. IV.

*Electronic address: srazzaque@uj.ac.za

†Electronic address: lili.yang@ung.si

II. NEUTRINO FLUX MODELS

A. Flux from individual bursts

We adopt the neutrino flux model from an adiabatic blastwave in constant density interstellar medium described in Ref. [21]. Cosmic rays (assumed protons) are accelerated in the forward shock in this scenario to a maximum energy of

$$E_{p,s} = 2.3\times10^{20}\,\frac{n_0^{1/8}\epsilon_{B,-1}^{1/2}E_{55}^{3/8}}{\phi(1+z)^{7/8}t_2^{1/8}}\ \mathrm{eV}, \quad (1)$$

where the isotropic-equivalent kinetic energy of the blastwave is $E_k = 10^{55}E_{55}$ erg, n_0 is the number density of particles per cubic centimeter in the circumburst medium, the fraction of shock energy converting to magnetic field energy is $\epsilon_B = 0.1\epsilon_{B,-1}$ and $\phi^{-1} \lesssim 1$ is an efficiency factor for proton acceleration. This energy is evaluated at a time $t = 10^2 t_2$ s after the GRB explosion and is valid for a time after the blastwave deceleration time scale

$$t_{dec} = 33.3\,\frac{(1+z)E_{55}^{1/3}}{n_0^{1/3}\Gamma_{2.5}^{8/3}}\ \mathrm{s}, \quad (2)$$

where the initial bulk Lorentz factor of the blastwave, before deceleration, is assumed $\Gamma_0 = 10^{2.5}\Gamma_{2.5}$. The flux of this cosmic-ray protons (if escape freely from the blastwave) can be calculated, assuming an E_p^{-2} spectrum arising from a shock-acceleration process, as

$$E_p^2 J_p(E_p) = 4.8\times10^{-9}\,\frac{(1+z)^{1/4}\epsilon_p n_0^{1/4}E_{55}^{3/4}}{\xi_1 t_2^{1/4}d_{28}^2}\ \mathrm{GeV\ cm^{-2}\ s^{-1}}, \quad (3)$$

where $\epsilon_p \lesssim 1$ is the fraction of blastwave kinetic energy carried by the shock-accelerated protons, $\xi = 10\xi_1$ is a spectral correction factor and a luminosity distance of $10^{28}d_{28}$ cm was assumed for the GRB. The total energy in cosmic rays is $\mathcal{E}_{CR} = \epsilon_p E_k/2$. Note that we have assumed ϵ_p to be a free parameter in our calculation, as there is no observational evidence yet to constrain it. Neutrino detection from GRBs in principle can be used to put constraint on ϵ_p.

The opacity for $p\gamma$ interactions of these protons with forward-shock afterglow synchrotron photons can be estimated as

$$\tau_{p\gamma}(E_{p,l}) = 0.7\,\frac{\epsilon_{B,-1}^{1/2}n_0E_{55}^{1/2}t_2^{1/2}}{(1+z)^{1/2}}, \quad (4)$$

at an energy

$$E_{p,l} = \frac{1.3\times10^8\,t_2^{3/4}}{(1+z)^{7/4}\epsilon_{B,-1}^{1/2}\epsilon_{e,-1}^2 n_0^{1/4}E_{55}^{1/4}}\ \mathrm{GeV}, \quad (5)$$

which corresponds to the break energy in the afterglow synchrotron spectrum due to the characteristic synchrotron photon energy $h\nu_m$ of minimum-energy electrons [27]. Here $\epsilon_e = 0.1\epsilon_{e,-1}$ is the fraction of shock energy converting to accelerated electrons in the blastwave. Another break appears in the opacity curve due to the characteristic synchrotron photon energy $h\nu_c$ of cooling electrons and is given by

$$E_{p,h} = 1.0\times10^{12}\,\frac{\epsilon_{B,-1}^{3/2}n_0^{3/4}E_{55}^{3/4}}{(1+z)^{3/4}t_2^{1/4}}\ \mathrm{GeV}. \quad (6)$$

Note that $\tau_{p\gamma}$ and $E_{p,l}$ increase while $E_{p,s}$ and $E_{p,h}$ decrease with time. These competing factors determine an energy range $E_{p,l} < E_p < \min\{E_{p,s}, E_{p,h}\}$ in which $p\gamma$ interaction is the most efficient.

In the case of fast-cooling afterglow synchrotron spectrum [27], $h\nu_c < h\nu_m$, the $p\gamma$ opacity scales with proton energy as

$$\tau_{p\gamma}(E_p) = \tau_{p\gamma}(E_{p,l}) \times \begin{cases} \left(\frac{E_p}{E_{p,l}}\right)^{k/2}; E_p \lesssim E_{p,l} \\ \left(\frac{E_p}{E_{p,l}}\right)^{1/2}; E_{p,l} \lesssim E_p \lesssim E_{p,h} \\ \left(\frac{E_{p,h}}{E_{p,l}}\right)^{1/2}; E_p \gtrsim E_{p,h}, \end{cases} \quad (7)$$

where $k = 2.5$ is the electron spectrum typically used for synchrotron afterglow modeling [27], which is consistent with modeling of X-ray afterglow data from Swift-XRT observations of a large number of GRBs [28]. On the other hand, in the case of slow-cooling afterglow synchrotron spectrum, $h\nu_c > h\nu_m$, the $p\gamma$ opacity scales as

$$\tau_{p\gamma}(E_p) = \tau_{p\gamma}(E_{p,l}) \times \begin{cases} \left(\frac{E_{p,h}}{E_{p,l}}\right)^{k/2-1/2}\left(\frac{E_p}{E_{p,h}}\right)^{k/2}; E_p \lesssim E_{p,h} \\ \left(\frac{E_p}{E_{p,l}}\right)^{k/2-1/2}; E_{p,h} \lesssim E_p \lesssim E_{p,l} \\ 1; E_p \gtrsim E_{p,l}. \end{cases} \quad (8)$$

The transition from fast-cooling to slow-cooling spectra happens when $h\nu_c = h\nu_m$ or $E_{p,h} \approx E_{p,l}$ at a time

$$t_0 = 1.1\times10^7\,(1+z)\epsilon_{B,-1}^2\epsilon_{e,-1}^2 n_0 E_{55}\ \mathrm{s}. \quad (9)$$

To calculate neutrino fluxes from $p\gamma$ interactions, we calculate an intermediate charged pion flux given by

$$J_\pi(E_\pi) \approx \frac{1}{2\langle x\rangle}J_p\left(\frac{E_\pi}{\langle x\rangle}\right) \times \min\left\{\tau_{p\gamma}\left(\frac{E_\pi(1+z)}{\langle x\rangle\Gamma}\right), 3\right\}, \quad (10)$$

where $\langle x\rangle \approx 0.2$ is the mean inelasticity for $p\gamma \to \pi$ production through delta resonance. Finally, the neutrino fluxes from pion decay are calculated by integrating over the product of pion flux and various scaling functions for

the $\pi^+ \to \mu^+\nu_\mu \to e^+\nu_e\bar{\nu}_\mu\nu_\mu$ chain decay [30]. As for example, π^+ decay ν_μ flux is

$$J_{\nu_\mu}(E_\nu) = \int_0^1 \frac{dx}{x}\frac{\Theta(1-r_\pi-x)}{1-r_\pi} J_\pi\left(\frac{E_\nu}{x}\right) \qquad (11)$$

where $x = E_\nu/E_\pi$, $r_\pi = m_\mu^2/m_\pi^2$ and Θ is a Heaviside step function. More details can be found in Ref. [21].

Neutrino fluxes from GRB blastwave last for a very long time [21], essentially until all kinetic energy is dissipated. The intensity, however, progressively decreases over time. We calculate ν fluxes until a time when the blastwave essentially becomes non-relativistic with a Lorentz factor

$$\Gamma \sim 1\,\frac{(1+z)^{3/8}E_{55}^{1/8}}{n_0^{1/8}t_{7.5}^{3/8}} \qquad (12)$$

after one year time scale, $t = 10^{7.5}t_{7.5}$ s. Note that the dependence of this time scale on E_k and n_0 is rather mild. For the Lorentz factor $\Gamma \gtrsim \theta_{\rm jet}^{-1} \approx 14(\theta_{\rm jet}/0.06)$, where $\theta_{\rm jet}$ is the GRB jet opening angle, the photon density in the blastwave decreases rapidly at late time [29, 31]. We found, however, no significant change in the time-intgrated flux or fluence as the fluence is dominated by flux at earlier time (see Ref. [21] and Fig. 2 therein).

Figure 1 shows time integrated $\nu_\mu + \bar{\nu}_\mu$ energy flux (after oscillation over astrophysical distance) or fluence $E_\nu^2 S_\nu$ evaluated for different blastwave kinetic energies, $E_k = 10^{51}$–10^{55} erg, (in different panels) and for different redshift, $z = 0.3$–9.0, (as different lines in each panel). We have assumed that $t_{dec} = 10$ s in Eq. (2) is fixed for all GRBs and is determined by Γ_0 as we have kept all other parameters fixed. The maximum integration time is determined by Eq. (12). Note that the E_ν at which the fluence curves peak is primarily determined by the proton break energy $E_{p,l}$ in Eq. (5), above which $p\gamma$ opacity becomes significant and the maximum proton energy $E_{p,s}$ in Eq. (1), above which the proton spectrum drops exponentially.

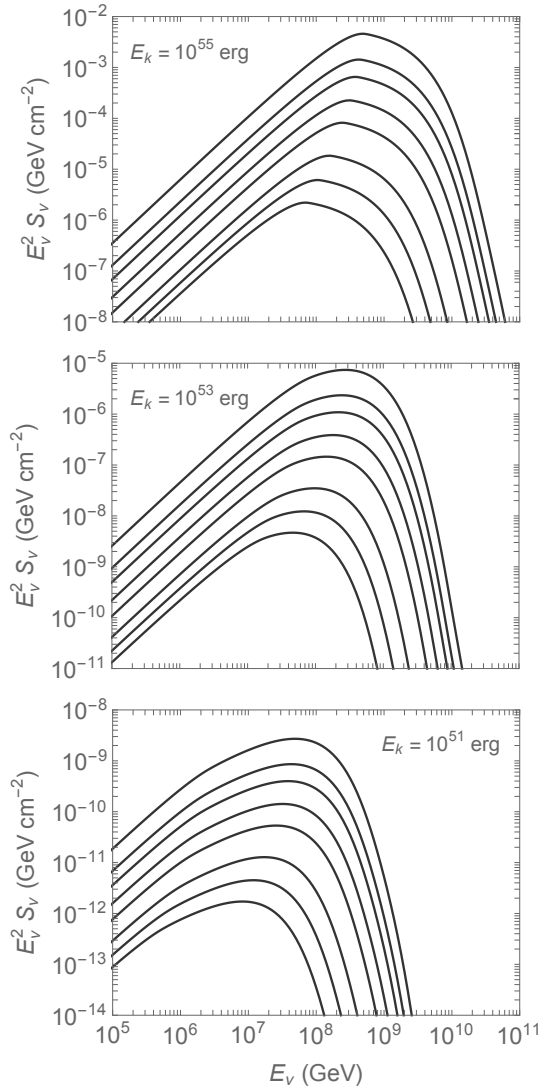

FIG. 1: Neutrino energy fluence ($\nu_\mu + \bar{\nu}_\mu$ after oscillation over astrophysical distances) from GRB blastwaves at redshift $z =$ 0.3, 0.5, 0.7, 1.1, 1.7, 3.3, 5.5, 9.0 from top to bottom curves in each panel. The top, middle and bottom panels correspond to $E_k = 10^{55}$ erg, 10^{53} erg and 10^{51} erg of isotropic-equivalent kinetic energy, respectively, of the blastwave in an interstellar medium of constant particle density $n_0 = 1$ cm^{-3}.

B. Diffuse neutrino flux

We calculate diffuse GRB blastwave neutrino flux by integrating fluence of individual bursts over the kinetic energy and redshift distributions of the observed rate of long-duration GRBs. We assume that the isotropic-equivalent kinetic energy is given by

$$E_k = \eta t L_\gamma \qquad (13)$$

where L_γ is the isotropic-equivalent γ-ray luminosity of long GRBs, $t \sim 10$ s is the typical duration of long GRBs and η is a dimensionless baryon-loading factor. We take $\eta t = 40$ s in our calculation as a parameter, following evidences for $\sim 20\%$ radiation efficiency for all GRBs [31] and typical ~ 10 s duration of long GRBs.

Given a rate of long duration GRBs, $\dot{n}_{\rm GRB}(z, L)$ per unit comoving volume element and per unit luminosity interval, the diffuse neutrino flux can be derived as [32]

$$J_\nu(E_\nu) = \frac{1}{16\pi^2}\int_{z_1}^{z_2}\frac{dz}{1+z}\frac{dV_c}{dz} \times \int_{L_1}^{L_2} dL\,\dot{n}_{\rm GRB}(z,L)S_\nu(E_\nu,z) \qquad (14)$$

where the comoving volume element is given by

$$\frac{dV_c}{dz} = \frac{4\pi c}{1+z}\left|\frac{dt}{dz}\right| d_L^2,$$

with cosmic time and redshift relation

$$\frac{dt}{dz} = \frac{-1}{H_0(1+z)\sqrt{\Omega_m(1+z)^3+\Omega_\Lambda}}$$

and luminosity distance

$$d_L = c(1+z)\int_0^z dz'(1+z')\frac{dt}{dz'}.$$

We use $H_0 = 69.6$ km s^{-1} Mpc^{-1}, $\Omega_M = 0.286$ and $\Omega_\Lambda = 0.714$ from the latest Planck results [33]. The upper and lower redshift values in Eq. (14) are set as $z_2 = 9.0$ and $z_1 = 0.1$, based on observations of long GRBs. The luminosity range is also set from observations as $L_2 = 2.5\times10^{53}$ erg/s and $L_1 = 2.5\times10^{49}$ erg/s.

A recent fit to the *Swift* GRB data with redshift information resulted in a luminosity function for long GRBs given by [34]

$$\phi(L) = \begin{cases} \left(\frac{L}{L_\star}\right)^{-0.17}; & L < L_\star \\ \left(\frac{L}{L_\star}\right)^{-1.44}; & L \geq L_\star, \end{cases} \quad (15)$$

where $L_\star = 10^{52.53}$ erg/s. The corresponding redshift evolution of GRB rate per unit comoving volume is

$$R(z) = R_0 \begin{cases} (1+z)^{2.07}; & z \leq 3.11 \\ (1+z)^{-1.36}4.11^{3.43}; & z > 3.11 \end{cases} \quad (16)$$

where $R_0 = 1.25$ Gpc^{-3} yr^{-1} is the local GRB rate density. Therefore,

$$\dot{n}_{\rm GRB}(z,L) = R(z)\phi(L). \quad (17)$$

Figure 2 shows diffuse GRB blastwave $\nu_\mu + \bar{\nu}_\mu$ flux after oscillation over astrophysical distances (shaded orange band) for two different circumburst particle densities, $n_0 = 1$ cm^{-3} (bottom curve) and 10 cm^{-3} (upper curve). A larger value of n_0 results in a lower proton break energy $E_{p,l}$ in Eq. (5) as well as a larger $p\gamma$ opacity in Eq. (4). As a result the flux for $n_0 = 10$ cm^{-3} is higher and peaks at a lower energy. Also shown in Fig. 2 are average atmospheric neutrino flux using a model in Ref. [35], recently detected IceCube cosmic neutrino flux (labeled "IC-cosmic") [36], as well as limits on diffuse flux from the Auger Observatory [37], ANITA-II [38] and RICE [39]. IceCube limits [11] on prompt GRB neutrino flux is labeled as "IC-GRB" while "Waxman-Bahcall" limit is based on observed UHECR flux [36, 40]. We also show cosmogenic neutrino flux models in Ref. [41], denoted as "GZK-p" and "GZK-Fe" in case UHECR primaries are proton and iron, respectively.

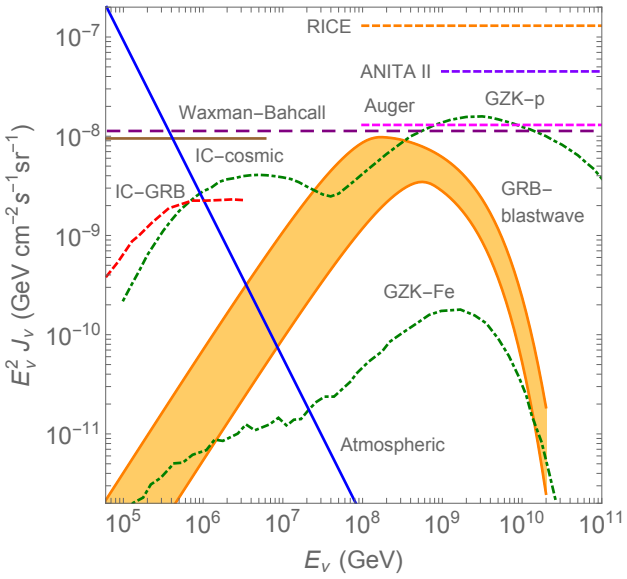

FIG. 2: Models of diffuse $\nu_\mu + \bar{\nu}_\mu$ fluxes from the GRB blastwave (shaded orange), atmosphere (solid blue) [35], GZK p-dominated (upper dot-dashed green) and GZK Fe-dominated (lower dot-dashed green) [41]. Also shown are the best-fit flux for the IceCube detected events (solid brown) [36], Waxman-Bahcall theoretical upper limit on the GZK flux [36, 40], IceCube upper limit on the prompt GRB flux [11]. Upper limits on diffuse $\propto E^{-2}$ flux from the Pierre Auger Observatory [37], ANITA-II [38] and RICE [39] experiments.

III. DETECTION RATES

Detection of PeV–EeV neutrinos from GRBs could be possible by the IceCube Neutrino Observatory, the largest operating neutrino telescope, by the Pierre Auger Observatory, the largest cosmic ray detector, and by future facilities such as the high-energy extension of IceCube, called IceHEX [26], the Askary'an Radio Array (ARA) [42] and ARIANNA [43]. Here we discuss prospects for detection of EeV neutrinos from individual GRBs at low redshift and from a diffuse flux from GRBs in the history of the universe.

A. Individual GRBs

Neutrinos from individual GRBs at low redshift and high γ-ray luminosity, which have higher fluxes at the Earth, could be detected. The expected number of GRBs within redshift z_0 and within a luminosity interval $L_1 \leq L \leq L_2$ can be calculated from the rate in Eq. (17) as,

$$R_{\rm GRB}(z_0) = \int_0^{z_0} \frac{dz}{1+z}\frac{dV_c}{dz}\int_{\log L_1}^{\log L_2} d\log L\, \dot{n}_{\rm GRB}(z,L). \quad (18)$$

Figure 3 shows this rate as a function of redshift for different intervals of E_k, the isotropic-equivalent blastwave kinetic energy, related to the GRB isotropic-equivalent γ-ray luminosity L according to Eq. (13). For example, the rate of GRBs with E_k in the 10^{54}–10^{55} erg is 1 yr^{-1} within $z_0 \approx 0.2$.

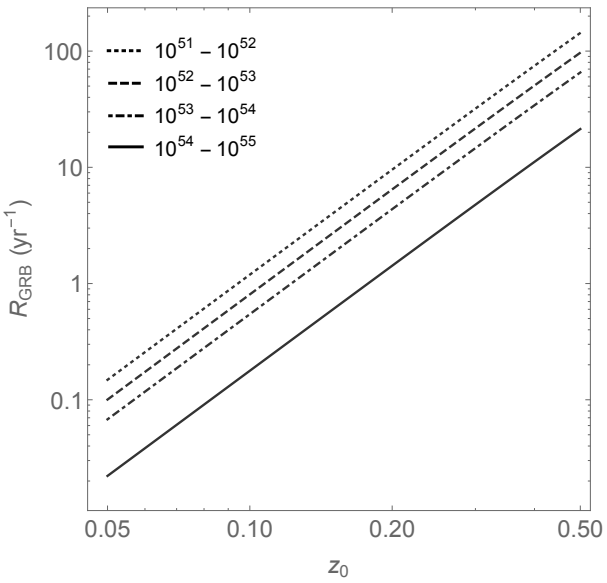

FIG. 3: The cumulative GRB rate [Eq. (18)] as a function of redshift z_0 for different intervals of isotropic-equivalent blast-wave kinetic energy E_k in erg.

Note that the Earth is essentially opaque to EeV neutrinos crossing a significant fraction of its diameter. As a result, neutrino telescopes are sensitive to downgoing neutrinos at EeV energies which reduces the observable GRB rate by approximately half.

Individual GRBs appear as point sources to the neutrino telescopes. The number of neutrino events of a particular neutrino flavor α from individual GRBs can be calculated as

$$N_{\rm evt,\alpha} = \int_{E_{\nu 1}}^{E_{\nu 2}} dE_\nu \, A_{\rm eff,\alpha}(E_\nu) S^{\rm GRB}_{\nu_\alpha}(E_\nu), \qquad (19)$$

where $A_{\rm eff,\alpha}$ is the effective area of the detector. In principle, $A_{\rm eff,\alpha}$ also depends on the zenith angle from the detector. Here we take an average value over 4π solid angle for IceCube [44]. We chose the width of the energy bins by considering the energy resolution of ~ 0.3-0.4 and 0.18 in $\log(E/{\rm GeV})$ scale for track like and cascade like events, respectively, in IceCube [45].

At EeV energies, the background essentially is the expected diffuse GZK neutrinos. The rate of these background events can be estimated as

$$N_{\rm bkg,\alpha} = 2\pi \frac{\delta\theta^2}{2} T \int_{E_{\nu 1}}^{E_{\nu 2}} dE_\nu \, A_{\rm eff,\alpha}(E_\nu) J^{\rm GZK}_{\nu_\alpha}(E_\nu), \quad (20)$$

where $\delta\theta$ is the angular resolution of the detector, assumed to be small, and T is the exposure time related to the GRB flux duration time.

We calculate the expected neutrino events from individual GRBs and backgrounds using IceCube effective areas [44] and $\delta\theta \sim 1^\circ$ angular resolutions for ν_μ and $\delta\theta \sim 10^\circ$ angular resolutions for ν_e or ν_τ. For definiteness we place the GRB at $z = 0.2$ with $E_k = 10^{55}$ erg. The rate of such GRBs is ~ 1 yr^{-1} (see Fig. 3). Figure 4 shows ν_e, ν_μ and ν_τ event distributions, both for the cases of 1 cm^{-3} and 10 cm^{-3} density of GRB circumburst medium. We also show the distributions of background events in Fig. 4. These background events have been calculated using atmospheric [35], and GZK-p and GZK-Fe flux models [41]. As can be seen, the background event

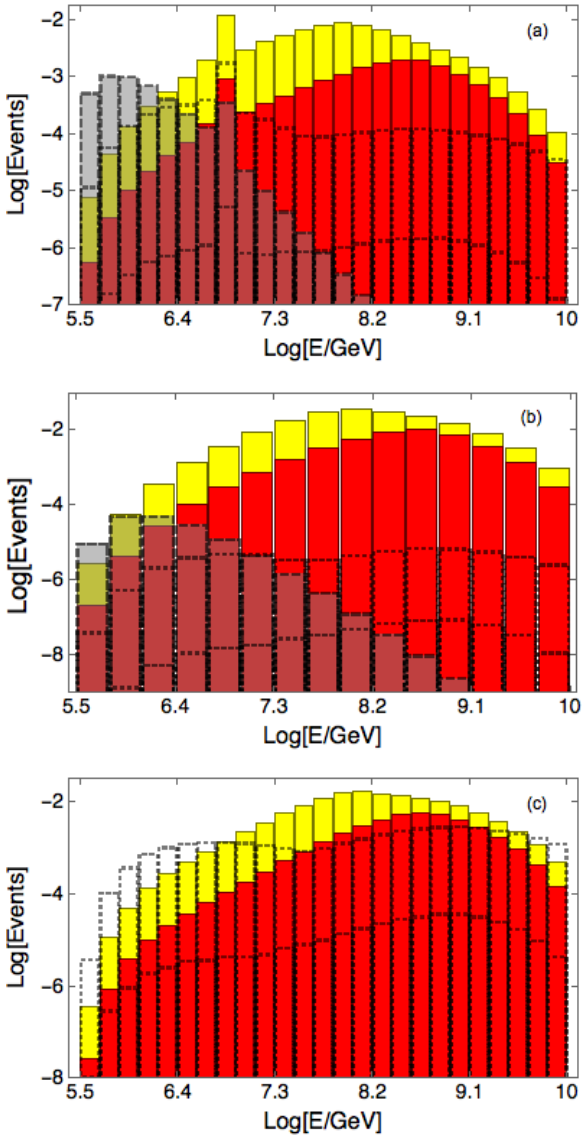

FIG. 4: Expected energy distributions of neutrino and antineutrino events in IceCube from a GRB at redshift 0.2 with an interstellar medium of constant particle density 1 cm^{-3} (red, solid edge, lower) and 10 cm^{-3} (yellow, solid edge, higher). Also shown are the background event distributions from atmospheric (shaded, dashed edge), GZK-p dominated (transparent, dotted edge, higher) and GZK-Fe dominated (transparent, dotted edge, lower) fluxes. The top, middle and bottom panels are for e-, μ- and τ-flavors respectively.

TABLE I: The expected number of ν_μ events from a GRB at $z = 0.2$ and from backgrounds as plotted in Fig. 4.

$\log(E/\mathrm{GeV})$	5.5-7	7-8.5	8.5-10
GRB $1/\mathrm{cm}^{-3}$	4.29×10^{-4}	2.00×10^{-2}	2.33×10^{-2}
GRB $10/\mathrm{cm}^{-3}$	5.47×10^{-3}	0.12	4.88×10^{-2}
Atmospheric	1.47×10^{-4}	6.36×10^{-6}	1.20×10^{-8}
GZK-Fe	3.24×10^{-8}	1.92×10^{-7}	2.71×10^{-7}
GZK-p	1.11×10^{-5}	2.12×10^{-5}	2.52×10^{-5}

rates are extremely low. The enhancement of ν_e events at ~ 6.3 PeV is due to enhancement of the effective area for Glashow resonance in the $\bar{\nu}_e$ cross section. Note that we have used an exposure time of 1 yr, a time scale when the GRB blastwave becomes non-relativistic [Eq. (2)].

Table I shows ν_μ track events in Fig. 4 for larger energy bins. As expected from flux models, the number of events is larger for 10 cm^{-3} density. Note that the prospect for detection of individual GRBs by IceCube is better for a GRB at $z < 0.2$ and with $E_k > 10^{55}$ erg. The rate of such GRBs is 1 per $\sim$ 5–10 yr (see Fig. 3). We will comment on the detectability of individual GRBs by a future high-energy extension of the IceCube, called IceHEX [26], in Sec. III C.

B. Neutrinos from diffuse flux

The number of ν events from diffuse GRB or background fluxes, $J^{\rm diff}_{\nu_\alpha}$, can be calculated as

$$N_{\mathrm{evt},\alpha} = 4\pi T \int_{E_{\nu 1}}^{E_{\nu 2}} dE_\nu \, A_{\mathrm{eff},\alpha}(E_\nu) J^{\rm diff}_{\nu_\alpha}(E_\nu), \qquad (21)$$

where $A_{\mathrm{eff},\alpha}$ is the average effective area over 4π solid angle [44] as noted before and T is the exposure time.

Figure 5 shows energy distributions of neutrino events in IceCube for different flavors from diffuse GRB neutrino fluxes and from backgrounds plotted in Fig. 2. We have used 10 yr exposure time for this calculation. While the background events from GZK-p flux [41] dominate most of the energy range, events from difuse GRB flux are above all backgrounds in the $\sim 10^{7.5}$-10^8 GeV range in case of 10 cm^{-3} density of the GRB circumburst medium. Table II lists the number of events in larger energy bins and for 5 year IceCube exposure. Note that detection of diffuse GRB blastwave neutrino flux is most probable in case the UHECR primaries are Fe, as suggested by the Pierre Auger Observatory [46]. In such a case UHE protons accelerated in the GRB blastwaves will not contribute significantly to the observed UHECR flux.

The Pierre Auger Observatory is sensitive to EeV neutrinos. The current limit on E^{-2} diffuse flux from the Pierre Auger Observatory [37] is the most stringent in the 0.1–100 EeV range, however it does not constrain the diffuse GRB blastwave flux models presented in this work (see Fig. 2).

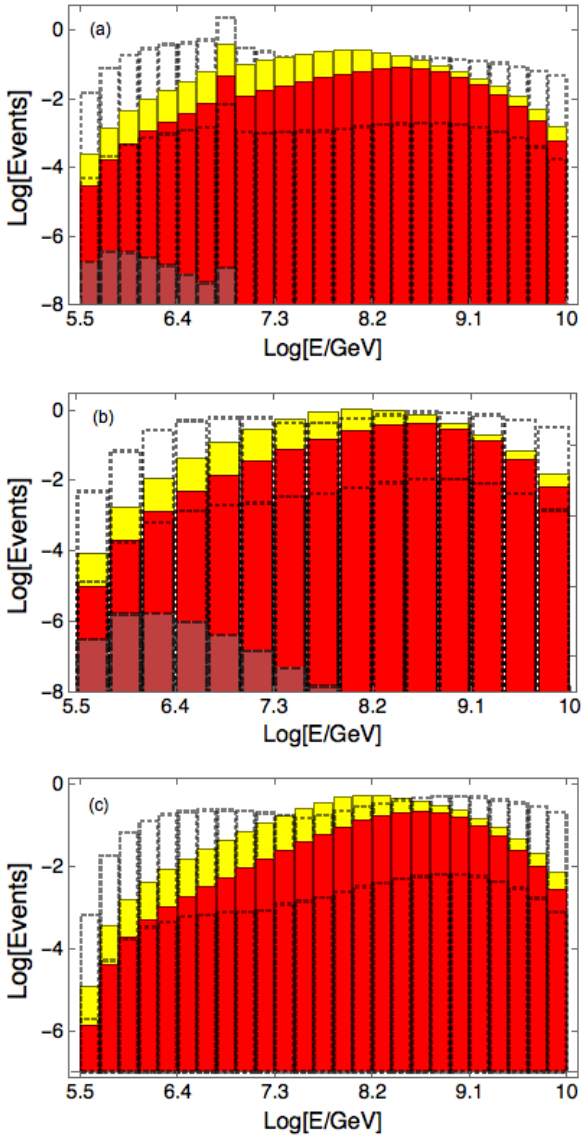

FIG. 5: Expected energy distributions of diffuse neutrino and antineutrino events in IceCube from GRBs with an interstellar medium of constant particle density 1 cm^{-3} (red, solid edge, lower) and 10 cm^{-3} (yellow, solid edge, higher). Distributions for atmospheric (shaded, dashed edge), GZK-p dominated (transparent, dotted edge, higher) and GZK-Fe dominated (transparent, dotted edge, lower) flux models are also shown. Events are calculated for 10 years of IceCube running time for e- (top panel), μ- (middle panel) and τ- (bottom panel) flavors.

C. Detectability by Future Neutrino Telescopes

There are several large, with $\gtrsim$ 100 km^2 geometric area, neutrino telescopes currently at the proposal stage [26, 42, 43]. The threshold energy for these detectors is expected to be in the $\sim$ 10-100 PeV range. The prospect for GRB blastwave neutrino detection by these large scale neutrino telescopes is very promising. Here we estimate

TABLE II: The expected event numbers for ν_e, ν_μ (in parentheses) and ν_τ (in brackets) from diffuse GRB fluxes and backgrounds in Fig. 2 for a 5-year IceCube search over the full sky.

$\log(E/\mathrm{GeV})$	5.5–7	7–8.5	8.5–10
GRB $1/\mathrm{cm}^{-3}$	0.03 (0.01) [0.01]	0.18 (0.44) [0.33]	0.13 (0.44) [0.43]
GRB $10/\mathrm{cm}^{-3}$	0.26 (0.09) [0.06]	0.83 (1.91) [1.40]	0.21 (0.71) [0.69]
Atmospheric	7.33×10^{-7} (2.50×10^{-6}) [—]	5.14×10^{-9} (1.08×10^{-7}) [—]	4.29×10^{-12} (2.04×10^{-10}) [—]
GZK-Fe	6.12×10^{-3} (2.12×10^{-3}) $[1.65\times10^{-3}]$	5.44×10^{-3} (1.26×10^{-2}) $[9.33\times10^{-3}]$	5.00×10^{-3} (1.78×10^{-2}) $[1.79\times10^{-2}]$
GZK-p	2.11 (0.73) [0.58]	0.67 (1.39) [0.99]	0.46 (1.66) [1.70]

event numbers for the proposed high-energy extension of IceCube [26], which we refer to as IceHEX, by extrapolating some characteristics of IceCube.

The effective area for a detector in case of downgoing neutrinos can be calculated, after taking into account ν survival probability and νN interaction probability within the detector, as [47, 48]

$$A_{\rm eff}(E_\nu) = 7\times10^{-5}\epsilon_{\rm det}A_{\rm geo}\left(\frac{E_\nu}{10^{4.5}\ \mathrm{GeV}}\right)^{\beta}, \qquad (22)$$

where $\beta = 1.35$ for $E_\nu < 10^{4.5}$ GeV while $\beta = 0.55$ for $E_\nu \geq 10^{4.5}$ GeV, $A_{\rm geo}$ is the geometric area of the detector and $\epsilon_{\rm det} < 1$ is a detector efficiency factor which is energy dependent in general. This parameterization reasonably reproduces the IceCube effective area with $A_{\rm geo} = 1$ km^2 and $\epsilon_{\rm det} \sim 0.1$ for $E_\nu \gtrsim 10^7$ GeV and for cascade events.

For IceHEX, we take the proposed geometric area $A_{\rm geo} = 100$ km^2 and fix $\epsilon_{\rm det} = 0.1$, the same as IceCube. For a GRB blastwave at $z = 0.2$, the expected number of cascade (ν_e and ν_τ) events are 10 and 40 for GRB circumburst density 1 cm^{-3} and 10 cm^{-3}, respectively, for $10^7 < E_\nu < 10^{10}$ GeV. Therefore neutrinos can be detected from a GRB blastwave up to a redshift $z \sim 0.5$. IceHEX will be able to detect diffuse flux of neutrinos from GRB blastwave as modeled in this work, at a rate of 20–100 cascade events/yr, depending on the flux level.

IV. DISCUSSION AND CONCLUSIONS

We have calculated neutrino fluence from GRB blastwaves in the PeV–EeV range, following Ref. [21] for individual GRBs (See Fig. 1). The detailed diffuse flux calculation is based on the observed rate of long GRBs and their redshift evolution. The diffuse flux per neutrino flavor peaks in the 0.1–1 EeV range (see Fig. 2) and is lower than the diffuse cosmic neutrino flux detected by IceCube [36], below 2 PeV. Our optimistic model of GRB blastwave neutrino flux peaks slightly below the Waxman-Bahcall limit [36, 40] and the conservative one is a factor 5 lower. Cosmogenic neutrino flux modeled in Ref. [41] with UHECR proton primary is higher than our model of GRB blastwave flux, except for our optimistic flux model and in the 0.03–0.3 EeV range. We do not require protons accelerated in the GRB blastwave to contribute to the observed UHECRs dominantly. Therefore if UHECRs are primarily heavy (iron) nuclei, our model of flux can dominantly contribute to the diffuse neutrino background in the PeV–EeV range.

We have also calculated neutrino events, using our diffuse flux model, in IceCube and future large neutrino telescopes referred to as IceHEX here, which is a planned high-energy upgrade of IceCube [26]. We find that IceCube can detect neutrinos from GRB blastwave after 5 years of operation if our diffuse flux model is correct. This would constitute detection of this flux component, in case UHECR primaries are heavy nuclei. In case UHECR primaries are protons, identification of the GRB blastwave diffuse flux component will take a longer time. With a 100 times larger effective area than IceCube at EeV energies, IceHEX can detect 20-100 cascade events/yr from GRBs if our diffuse flux model is valid.

Detection of neutrinos by current IceCube from an individual GRB blastwave may not be possible. Stacking analysis with individual GRBs, however, can improve the sensitivity. An observation strategy with long-term (~ 1 year time scale) monitoring of GRBs is needed. IceHEX will be able to detect 10's of events from an energetic GRB at $z = 0.2$ for which the rate is 1/yr (see Fig. 3). Since the neutrino events from individual GRBs are essentially background free, few events may constitute a detection and IceHEX may detect GRBs at redshift up to $z \sim 0.5$, where the rate is roughly 10 times higher. Such a detection will be crucial to understand GRB explosion energy, environment and most importantly acceleration of particles to ultrahigh energies.

Acknowledgments

This work was supported in part by the National Research Foundation (South Africa) grants nos. 87823 (CPRR) and 91802 (Blue Skies), to SR. We thank Kohta Murase for useful comments, in particular about the GRB jet break.

[1] E. Waxman, Phys. Rev. Lett. **75**, 386 (1995) [astro-ph/9505082].

[2] M. Vietri, Astrophys. J. **453**, 883 (1995) [astro-ph/9506081].

[3] X. Y. Wang, S. Razzaque and P. Meszaros, Astrophys. J. **677**, 432 (2008) [arXiv:0711.2065 [astro-ph]].

[4] P. Meszaros and M. J. Rees, Astrophys. J. **405**, 278 (1993).

[5] S. Razzaque, P. Meszaros and E. Waxman, Phys. Rev. D **68**, 083001 (2003) [astro-ph/0303505].

[6] E. Waxman and J. N. Bahcall, Phys. Rev. Lett. **78**, 2292 (1997) [astro-ph/9701231].

[7] D. Guetta, D. Hooper, J. Alvarez-Muniz, F. Halzen and E. Reuveni, Astropart. Phys. **20**, 429 (2004) [astro-ph/0302524].

[8] C. D. Dermer and A. Atoyan, Phys. Rev. Lett. **91**, 071102 (2003) [astro-ph/0301030].

[9] K. Murase and S. Nagataki, Phys. Rev. D **73**, 063002 (2006) [astro-ph/0512275].

[10] S. Hummer, P. Baerwald and W. Winter, Phys. Rev. Lett. **108**, 231101 (2012) [arXiv:1112.1076 [astro-ph.HE]].

[11] R. Abbasi *et al.* [IceCube Collaboration], Nature **484**, 351 (2012) [arXiv:1204.4219 [astro-ph.HE]].

[12] S. Adrián-Martínez, A. Albert, I. Al Samarai, M. André, M. Anghinolfi, G. Anton, S. Anvar and M. Ardid *et al.*, arXiv:1307.0304 [astro-ph.HE].

[13] M. G. Aartsen *et al.* [IceCube Collaboration], arXiv:1412.6510 [astro-ph.HE].

[14] B. Zhang and P. Kumar, Phys. Rev. Lett. **110**, no. 12, 121101 (2013) [arXiv:1210.0647 [astro-ph.HE]].

[15] M. Ackermann *et al.* [Fermi-LAT Collaboration], Science, **343**, 42 (2014)

[16] S. Gao, K. Kashiyama and P. Meszaros, Astrophys. J. **772**, L4 (2013) [arXiv:1305.6055 [astro-ph.HE]].

[17] N. Gehrels and S. Razzaque, Invited review article in the special issue of Frontiers of Physics on High Energy Astrophysics, eds. B. Zhang and P. Meszaros, arXiv:1301.0840 [astro-ph.HE].

[18] M. Ackermann, M. Ajello, K. Asano, M. Axelsson, L. Baldini, J. Ballet, G. Barbiellini and D. Bastieri *et al.*, Astrophys. J. Suppl. **209**, 11 (2013).

[19] C. D. Dermer, Astrophys. J. **574**, 65 (2002) [astro-ph/0005440].

[20] Z. Li, Z. G. Dai and T. Lu, Astron. Astrophys. **396**, 303 (2002) [astro-ph/0208435].

[21] S. Razzaque, Phys. Rev. D **88**, no. 10, 103003 (2013) [arXiv:1307.7596 [astro-ph.HE]].

[22] D. Xiao and Z. G. Dai, Astrophys. J. **790**, 59 (2014) [arXiv:1406.2792 [astro-ph.HE]].

[23] E. Waxman and J. N. Bahcall, Astrophys. J. **541**, 707 (2000) [hep-ph/9909286].

[24] Z. G. Dai and T. Lu, Astrophys. J. **551**, 249 (2001) [astro-ph/0002430].

[25] K. Murase, Phys. Rev. D **76**, 123001 (2007) [arXiv:0707.1140 [astro-ph]].

[26] J. Koskinen in "Neutrino Oscillation Workshop 2014," Conca Specchiulla (Otranto, Lecce, Italy), September 7-14, 2014; G. Hill in "Neutrino 2014," Boston, USA, June 1-7, 2014.

[27] R. Sari, T. Piran and R. Narayan, Astrophys. J. **497**, L17 (1998) [astro-ph/9712005].

[28] J. L. Racusin, E. W. Liang, D. N. Burrows, A. Falcone, T. Sakamoto, B. B. Zhang, B. Zhang and P. Evans *et al.*, Astrophys. J. **698**, 43 (2009) [arXiv:0812.4780 [astro-ph]].

[29] R. Sari, T. Piran and J. Halpern, Astrophys. J. **519**, L17 (1999) [astro-ph/9903339].

[30] P. Lipari, Astropart. Phys. **1**, 195 (1993).

[31] D. A. Frail, S. R. Kulkarni, R. Sari, S. G. Djorgovski, J. S. Bloom, T. J. Galama, D. E. Reichart and E. Berger *et al.*, Astrophys. J. **562**, L55 (2001) [astro-ph/0102282].

[32] S. Razzaque, P. Meszaros and E. Waxman, Mod. Phys. Lett. A **20**, 2351 (2005) [astro-ph/0509729].

[33] P. A. R. Ade *et al.* [Planck Collaboration], Astron. Astrophys. **571**, A16 (2014) [arXiv:1303.5076 [astro-ph.CO]].

[34] D. Wanderman and T. Piran, Mon. Not. Roy. Astron. Soc. **406**, 1944 (2010) [arXiv:0912.0709 [astro-ph.HE]].

[35] M. Honda, T. Kajita, K. Kasahara, S. Midorikawa and T. Sanuki, Phys. Rev. D **75**, 043006 (2007) [astro-ph/0611418].

[36] M. G. Aartsen *et al.* [IceCube Collaboration], Science **342**, 1242856 (2013) [arXiv:1311.5238 [astro-ph.HE]].

[37] J. Alvarez-Muniz in "Neutrino 2014," Boston, USA, June 1-7, 2014.

[38] P. W. Gorham *et al.* [ANITA Collaboration], Phys. Rev. D **85**, 049901 (2012) [arXiv:1011.5004 [astro-ph.HE], arXiv:1003.2961 [astro-ph.HE]].

[39] I. Kravchenko, S. Hussain, D. Seckel, D. Besson, E. Fensholt, J. Ralston, J. Taylor and K. Ratzlaff *et al.*, Phys. Rev. D **85**, 062004 (2012) [arXiv:1106.1164 [astro-ph.HE]].

[40] E. Waxman and J. N. Bahcall, Phys. Rev. D **59**, 023002 (1999) [hep-ph/9807282].

[41] K. Kotera, D. Allard and A. V. Olinto, JCAP **1010**, 013 (2010) [arXiv:1009.1382 [astro-ph.HE]].

[42] P. Allison, J. Auffenberg, R. Bard, J. J. Beatty, D. Z. Besson, S. Boser, C. Chen and P. Chen *et al.*, Astropart. Phys. **35**, 457 (2012) [arXiv:1105.2854 [astro-ph.IM]].

[43] S. W. Barwick, J. Phys. Conf. Ser. **60**, 276 (2007) [astro-ph/0610631].

[44] M. G. Aartsen *et al.* [IceCube Collaboration], Phys. Rev. Lett. **111**, 021103 (2013) [arXiv:1304.5356 [astro-ph.HE]].

[45] E. Resconi [IceCube Collaboration], Nucl. Instrum. Meth. A **602**, 7 (2009) [arXiv:0807.3891 [astro-ph]].

[46] J. Abraham *et al.* [Pierre Auger Collaboration], Phys. Rev. Lett. **104**, 091101 (2010) [arXiv:1002.0699 [astro-ph.HE]].

[47] S. Razzaque, P. Meszaros and E. Waxman, Phys. Rev. D **69**, 023001 (2004) [astro-ph/0308239].

[48] K. Ioka, S. Razzaque, S. Kobayashi and P. Meszaros, Astrophys. J. **633**, 1013 (2005) [astro-ph/0503279].

[49] Note that proton-proton (*pp*) interactions can be dominating in the GRB jet in its very early stage of evolution, while the jet is still burrowing through the stellar envelope and the density of material in the jet is very high [5]. During the time of prompt and afterglow emissions, the density of material is very low because of increased size of the jet and *pp* interactions become less important.